

ADVANCED FUNCTIONAL MATERIALS

Supporting Information

for *Adv. Funct. Mater.*, DOI: 10.1002/adfm.202213717

Self-Healing Photochromic Elastomer Composites for
Wearable UV-Sensors

Tiwa Yimyai, Daniel Crespy, and Abdon Pena-
Francesch**

Supporting Information

Self-healing photochromic elastomer composites for wearable UV-sensors

Tiwa Yimyai, Daniel Crespy, and Abdon Pena-Francesch**

* Corresponding Author. E-mail address: daniel.crespy@vistec.ac.th and abdon@umich.edu

Table of contents

Figure S1: Synthetic routes for the preparation of PUSH and PUHD polymers.

Figure S2: Photochromic mechanism and FTIR spectra of PUSH, PMA, and photoPUSH.

Figure S3: Color change of PMA deposited on different substrates after exposure to UVA light.

Figure S4: Ultraviolet–visible (UV–vis) light transmittance spectra of PUSH films.

Figure S5: UV absorbance of photoPUSH films as a function of UVA dose and temperature.

Figure S6: Color stability of photoPUSH for several days.

Figure S7: Reversible color transition of a photoPUSH composite.

Figure S8: UV absorbance at 760 nm as a function of UVA light for photoPUSH films.

Figure S9: Ultraviolet–visible (UV–vis) light transmittance spectra of melanin-mimicking UV filters.

Figure S10: Mechanical creep of PUSH films under UV light exposure.

Figure S11: Healed sample between PUSH (transparent) and photoPUSH (blue) after cutting.

Figure S12: Healing of a scratched “M”-shaped photoPUSH film at 70 °C.

Figure S13: PhotoPUSH UV-sensor attached to a window for natural sunlight exposure monitoring.

Figure S14: Cross-sectional view of cotton textile and PUSH/cotton textile.

Figure S15: PhotoPUSH UV detection wristband immersed into water. Healing of photoPUSH wristband.

Figure S16: Reversible photochromism of a self-healing SP/PUSH composite film.

Table S1: Benchmark of representative photoelectric wearable UV sensor technologies.

Table S2: Benchmark of representative photochromic wearable UV sensor technologies.

Table S3: Benchmark of commercial wearable UV sensor technologies.

Movie S1: Self-healing of PUHD & PUSH elastomers.

Movie S2: Multimaterial photoPUSH elastomer composites under different mechanical stress.

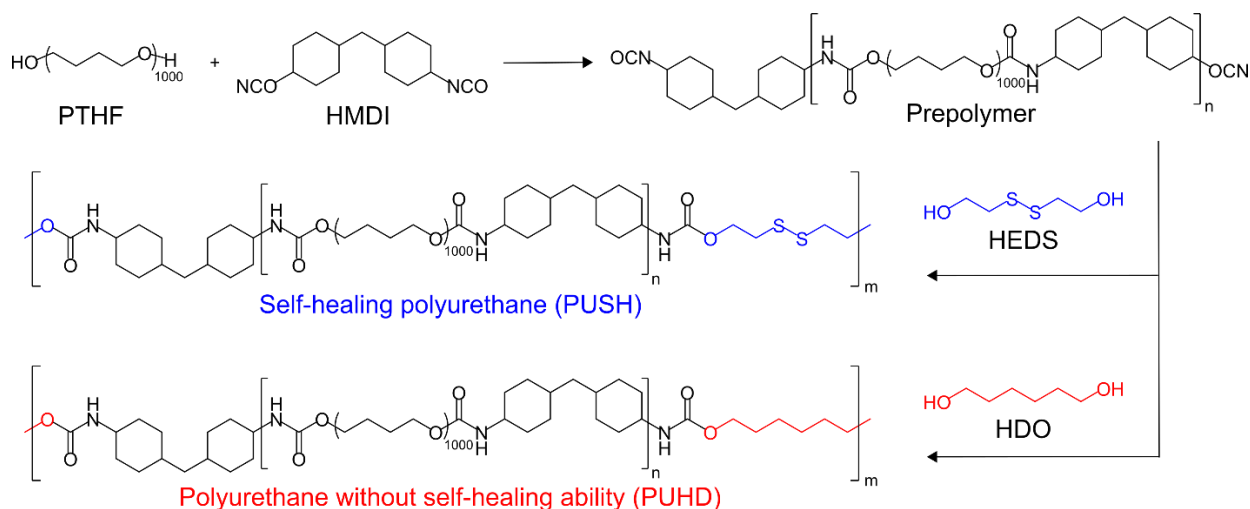


Figure S1. Synthetic routes for the preparation of self-healing polyurethane (PUSH) and polyurethane without self-healing ability (PUHD).

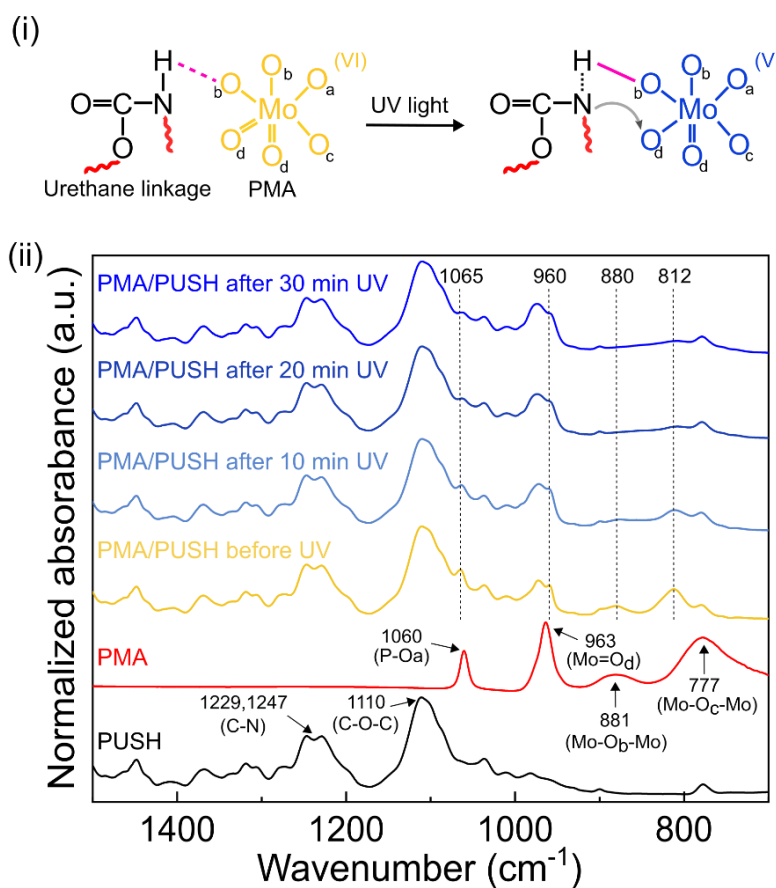


Figure S2. (i) A photochromic mechanism between phosphomolybdic acid hydrate (PMA) molecules and urethane linkages in a self-healing polymer network. (ii) FTIR spectra of PUSH polymer, PMA, and photoPUSH (5.7 wt% PMA) before and after being exposed to UVA light for 10–30 min.

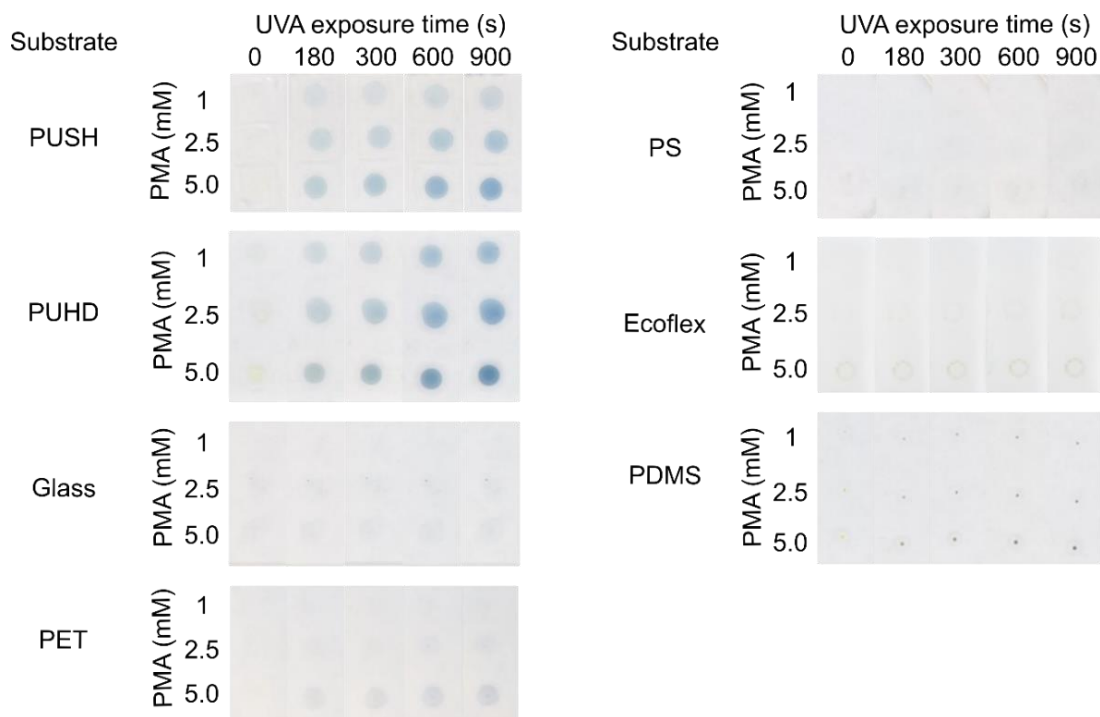


Figure S3. PMA deposited on different substrates, showing color change after exposure to UVA light at a wavelength of 368 nm with an increasing exposure time.

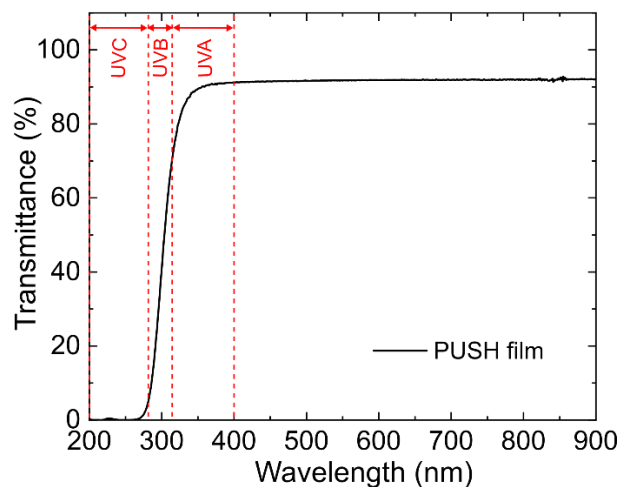


Figure S4. Ultraviolet–visible (UV–vis) light transmittance spectra of PUSH film (thickness = 0.09 mm).

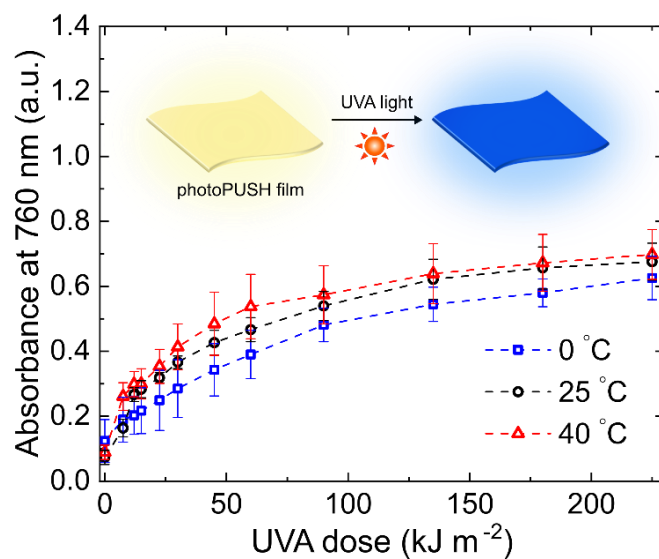


Figure S5. UV absorbance at a wavelength of 760 nm as a function of UVA light ($\lambda_{\text{max}} = 365$ nm) dose for photoPUSH films with 5.7 wt% PMA under different temperatures.

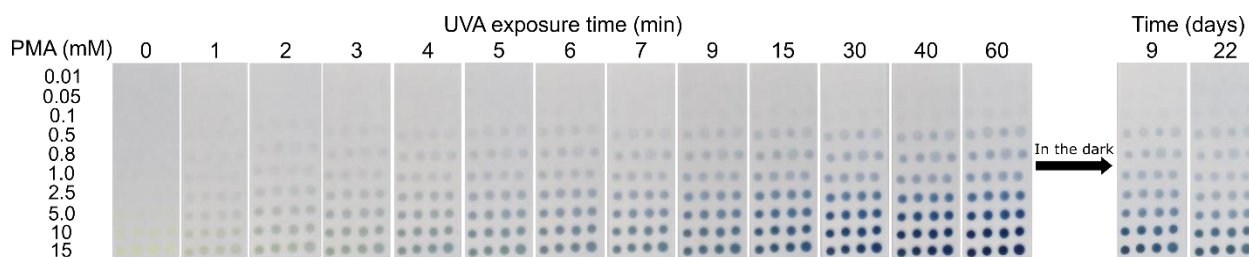


Figure S6. Photographs of a PUSH film with different amount of PMA after being irradiated under UVA and kept in the dark at 25 °C.

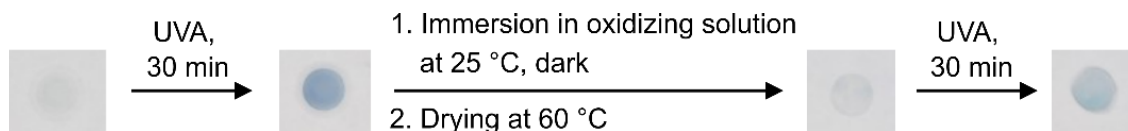


Figure S7. Photographs showing the reversible color transition of a photoPUSH composite with 11.4 wt% PMA upon oxidation with an aqueous solution of hydrogen peroxide.

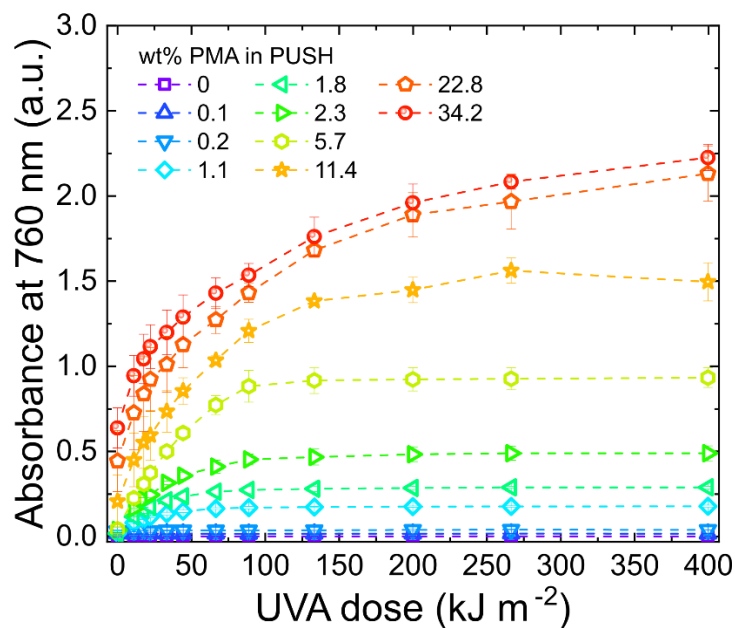


Figure S8. UV absorbance at a wavelength of 760 nm as a function of UVA light ($\lambda_{\max} = 368$ nm) dose for photoPUSH films with different PMA amounts.

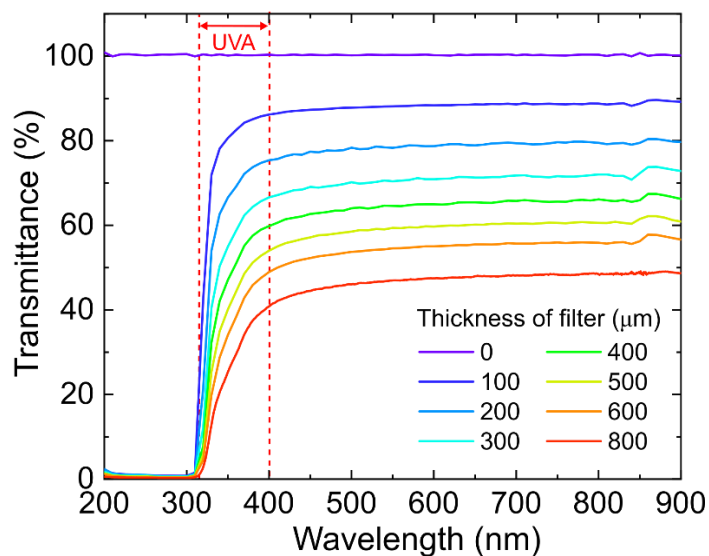


Figure S9. Melanin-mimic UV filters (polyethylene terephthalate (PET) thin films) with different thickness. The wavelength range for UVA, B, and C is marked with dash lines at 200–280 nm, 280–315 nm, and 315–400 nm, respectively.

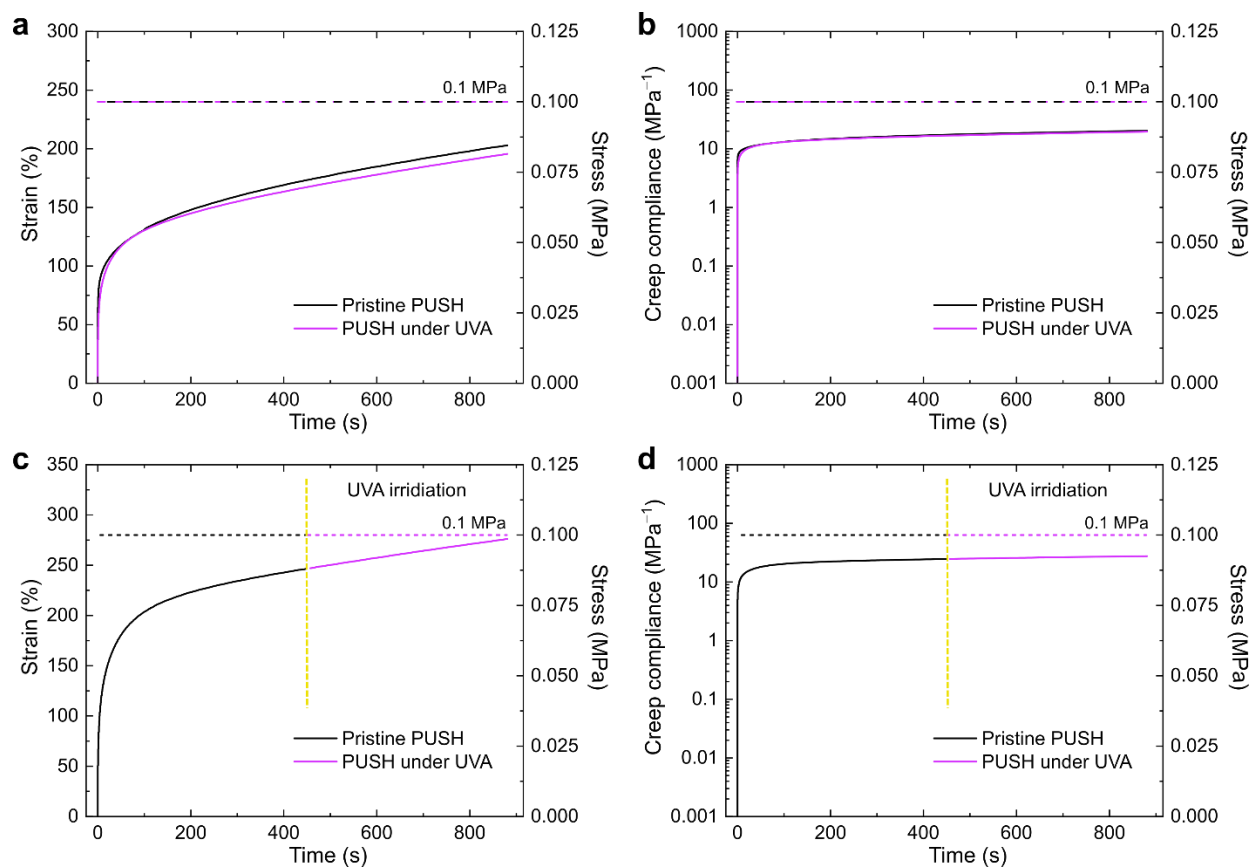


Figure S10. Comparison of shear strain (%) and creep compliance of (a,b) two different PUSH films and (c,d) a PUSH film under constant stress of 0.1 MPa with and without UV light exposure.

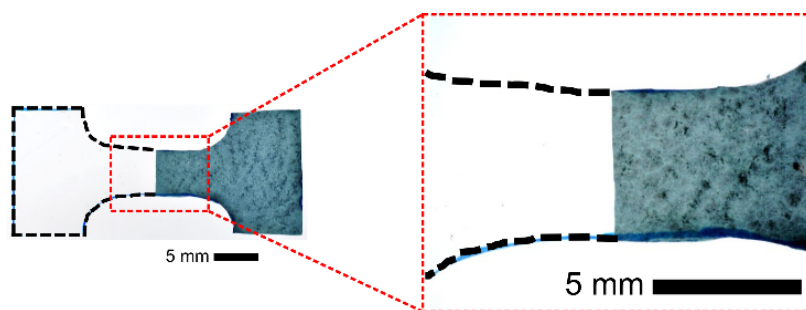


Figure S11. A photograph showing a healed dog-bone shaped sample between PUSH (transparent, in black dashed line region) and photoPUSH (blue). The magnified image on the right showed the healed position.

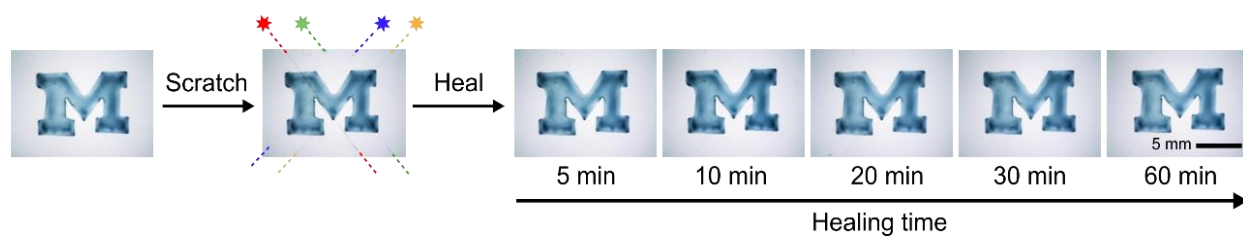


Figure S12. A “M”-shaped photoPUSH film was scratched and then healed at 70 °C for different healing times.

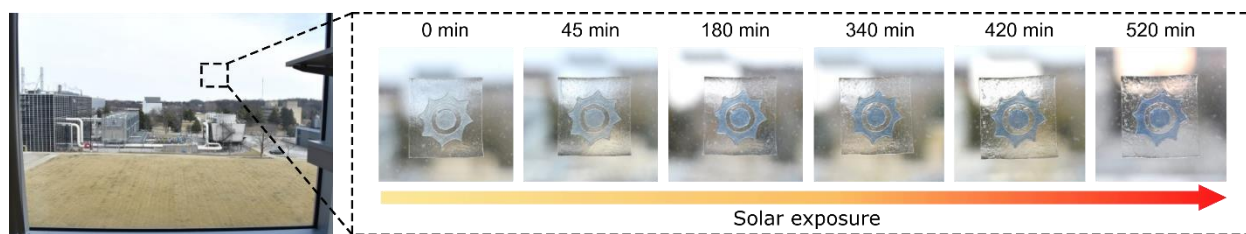


Figure S13. Photographs of a UV-sensor (photoPUSH composite on a PUSH sticker film) attached to a window for natural sunlight exposure monitoring.

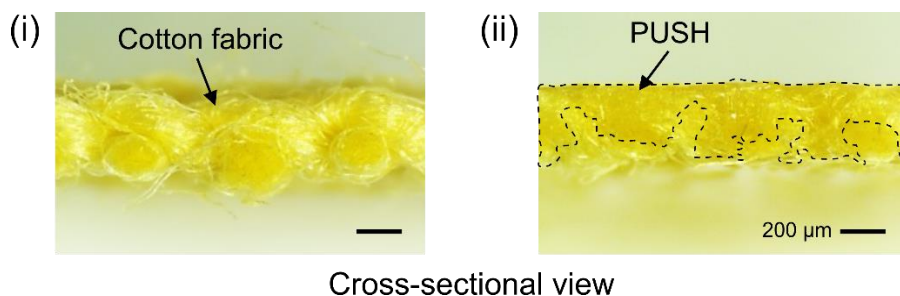


Figure S14. Optical images showing cross-sectional view of (i) original cotton textile and (ii) PUSH penetrating through the cotton textile.

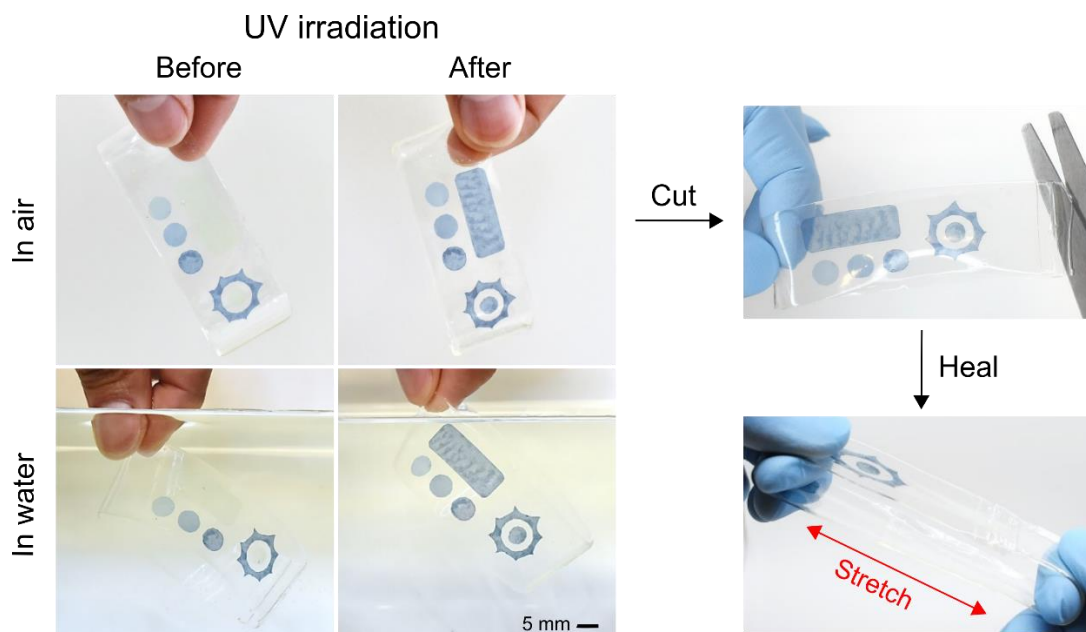


Figure S15. A UV detection wristband exhibits color change with UV light in air and in water. The wristband was cut and subsequently healed at 70 °C, recovering the mechanical and photochromic properties.

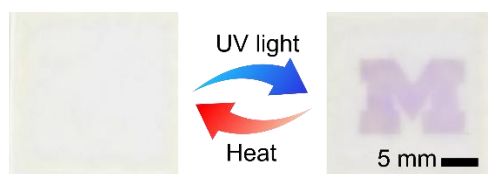


Figure S16. Reversible photochromism of a self-healing SP/PUSH composite film upon UVA light ($\lambda_{\max} = 365 \text{ nm}$) irradiation with a M-shaped photomask and heating at 60 °C.

Table S1. Benchmark of representative photoelectric wearable UV sensor technologies. Adapted from ref.^[1]

Fabrication			Specificity		Selectivity	Sensitivity		Real-time monitoring		Practical applicability					Ref
Functional materials	Substrates	Fabrication techniques	Visible blind	Detection wavelength	Spectral selectivity	Light intensity (mW cm ⁻²)	MED range	Intensity	Cumulative dose	Reusability	Naked eye detection ^a	Custom for different skin types	Stretchability	Self-healing ability	
ZnO/Graphene	Cellulose paper	ZnO pencil writing	✓	365 nm	✗	0.5–3.9	✓	✓	✗	✓	✗	✗	✗	✗	[2]
Te/ZnO, Te/TiO ₂	Paper	Brush writing	Partial	350 nm	✗	N/A	N/A	✓	✗	✓	✗	✗	✗	✗	[3]
ZnO	Paper	Screen printing	✗	254 nm	✗	3.8	✗	✓	✗	✓	✗	✗	✗	✗	[4]
ZnO	PI	Inkjet printing	✓	365 nm	✗	9.1 × 10 ⁻³	✓	✓	✗	✓	✗	✗	N/A	✗	[5]
ZnO/rGO	mica	Laser Writing	N/A	365 nm	✗	0.66–20.03	✓	✓	✗	✓	✗	✗	N/A (bending)	✗	[6]
p-CuZnS/n-TiO ₂	Ti wires	Chemical bath	✗	350 nm	✗	1.26	✓	✓	✗	✓	✗	✗	✗	✗	[7]
TiO ₂ /GO	Parylene-C	Spraying	Partial	270 nm	✗	0–2.5 × 10 ⁻²	✓	✓	✗	✓	✗	✗	N/A (bending)	✗	[8]
TiO ₂ /GO	Gold-on-glass interdigitated electrodes	AC electrophoresis deposition	Partial	Solar simulator	✗	3.2	✓	✗	✓	N/A	✗	✗	✗	✗	[9]
PANI/TST/PAG/CNTs	PI	Laser printing dip coating	✓	365 nm	✗	40	✓	✗	✓	✗	✗	✗	N/A (flexible)	✗	[10]
CNTs	Cellulose thread	Dip coating	✓	254, 365 nm	✓	2–4	✓	✓	✗	✓	✗	✗	N/A (flexible)	✗	[11]
CNTs	Glass, PI	Drop casting	N/A	254 nm	N/A	0.2–2	✗	✓	✗	✓	✗	✗	✗	✗	[12]
ZnO/SiO ₂ /TiO ₂	Glass	Direct deposition	✓	370 nm	✓	8.6 × 10 ⁻²	✓	✓	✗	✓	✗	✗	✗	✗	[13]
Photodiode arrays	Copper, PI	N/A	N/A	365, 305 nm	✓	2.2, 0.16	✓	✓	✓	✓	✗	App-customizable	✗	✗	[14]
Black phosphorus	SiO ₂ /Si, PEN, PI	N/A	✗	365, 208 nm	✓	2	✓	✓	✗	✓	✗	✗	✗	✗	[15]
PMA	Self-healing polyurethane	Solution blending/casting, assemblability	N/A	UVA, B, C (368, 365, 306, and 265 nm)	✓	2–5.6	✓	✗	✓	✓	✓	✓	✓	✓	This work

a) The “naked eye detection” here refers to the state where the sensor response is detectable directly by the eye and thus offers the user the sensing results without external interfaces.

Table S2. Benchmark of representative photochromic wearable UV sensor technologies. Adapted from ref.^[1]

Fabrication			Specificity		Selectivity	Sensitivity		Real-time monitoring		Practical applicability					Ref
Functional materials	Substrates	Fabrication techniques	Visible blind	Detection wavelength	Spectral selectivity	Light intensity (mW cm ⁻²)	MED range	Intensity	Cumulative dose	Reusability	Naked eye detection	Custom for different skin types	Stretchability	Self-healing ability	
C1H/MG, DPIC/TB	PVB	Spin coating	✓	Solar simulator	✗	UVI 5	✓	✗	✓	✗	✓	✗	✗	✗	[16]
PDPPS-TF/CVL PDPPS-TF/CR	PDMS	Screen printing	✓	UVA, UVB	✓	UVA 1.8 UVB 0.17	✓	✓	✓	✗	✗	✓	✓	✗	[17]
TiO ₂ /brilliant blue FCF/PVP	Photo paper	Inkjet printing	✓	Solar simulator	✗	3.2	✓	✗	✓	✗	✓	✓	✗	✗	[18]
TiO ₂ /RBBR/ glycerol	hydroxyethyl cellulose	Spin coating	✓	368 nm	✗	1.5	✓	✗	✓	✗	✓	✗	N/A	✗	[19]
Prussian Blue/TiO ₂	polyethylene terephthalate	Cyclic voltammetry	✓	365 nm	✗	0.2–10	N/A	✓	✗	✓	✓	✗	✗	✗	[20]
DTEC	LDPE	Solution casting	✗	Solar simulator	✓	100	✓	✗	✓	✗	✓	✗	✗	✗	[21]
PMA/LA	Filter paper	Pen writing	✓	UVA, B, C	✓	0.5	✓	✗	✓	✗	✓	✓	✗	✗	[22]
Hackmanite (Na,M) ₂ Al ₆ Si ₆ O ₂₄ (Cl,S) ₂	N/A	N/A	✗	Solar simulator	✓	UVI 0–6	✓	✓	✓	✓	✗	✗	✗	✗	[23]
UV-bleachable dye/LED	PDMS	Spin casting	✓	Solar simulator	✗	4.2	✓	✗	✓	N/A	✗	✗	✓	✗	[24]
PMA-ONB	PEN	Drop casting	N/A	Solar simulator	✗	100	✓	✗	✓	✗	✓	✗	N/A (bending)	✗	[25]
PMA	Self-healing polyurethane	Solution blending/casting, assemblability	N/A	UVA, B, C (368, 365, 306, and 265 nm)	✓	2-5.6	✓	✗	✓	✓	✓	✓	✓	✓	This work

Table S3. Benchmark of commercial wearable UV sensor technologies. Adapted from ref.^[1]

Category	Product	Format	Battery-free/Self-powered	UVA/UVB differentiation	Cumulative dose	Activation-free	Sunscreen applicable	Custom for different skin types	Reusable ^a	Water-proof	Work on its own	Stretchability	Self-healing ability	Ref
Electronic	Microsoft Band	Wristband	✗	✗	✗	✗	✗	✗	✓	✗	✓	✗	✗	[26]
Electronic	My skin track UV	Clip	✓	✓	✓	✓	✗	✓	✓	✓	✗	✗	✗	[27, 28]
Electronic	Shade	Magnetic clip	✗	✓	✓	✓	✗	✓	✓	✓	✗	✗	✗	[29]
Electronic	Sunsprite	Clip	✓	✗	✓	✓	✗	✗	✓	✗	✓	✗	✗	[30]
Electronic	Qsun	Clip	✗	✓	✓	✓	✗	✓	✓	✗	✓	✗	✗	[31]
Electronic	Stella	Wristband	✗	N/A	✓	✓	✗	✓	✓	✓	✓	✗	✗	[32]
Electronic	Violet	Clip	✗	✓	✓	✓	✗	✓	✓	✓	✓	✗	✗	[33]
Electronic	Sunfriend	wristband	✗	✗	✓	✓	✗	✓	✓	✓	✓	✗	✗	[34]
Colorimetric/ Electronic	My UV patch	Sticker	✓	App-differentiable	✓	✓	✓	App-customizable	✗	✓	✗	✗	✗	[27, 35]
Colorimetric	Sundicator	Sticker/wrist band	✓	✗	✗	✗	✓	✗	✗	✓	✓	✗	✗	[36]
Colorimetric	Smartsun	Sticker/wrist band	✓	✗	✗	✓	✓	✗	✗	✓	✓	✗	✗	[37]
Colorimetric	SPOTMYUV	Sticker	✓	✗	✗	✗	✓	✗	✗	✓	✓	✗	✗	[38]
Colorimetric	Logicink	Sticker	✓	✗	✓	✓	✓	✗	✗	✓	✓	N/A	✗	[39]
Colorimetric	photoPUSH	patch/sticker /wristband	✓	✓	✓	✓	✓	✓	✓	✓	✓	✓	✓	This work

a) Reusable is defined as the potential capability of the sensor to be reset and reused after the first day's usage, such that the previous exposure data does not affect the ongoing performance of the sensor.

Abbreviations

AC	Alternating current
CIH	Chloral hydrate
CNTs	Carbon nanotubes
CR	Congo red
CVL	Crystal violet lactone
DPIC	Diphenyliodonium chloride
DTEC	(2Z,6Z)-2,6-bis(2-(2,6-diphenyl-4H-thiopyran-4-ylidene)ethylidene) cyclohexanone
FCF	Brilliant blue FCF
GO	Graphene oxide
LA	Lactic acid
LDPE	Low-density polyethylene
LED	Light-emitting diode
MG	Malachite green
N/A	Not available
ONB	Ortho-nitrobenzyl
PAG	Photoacid generator
PANI	Polyaniline
PDMS	Polydimethylsiloxane
PDPPS-TF	4-phenoxyphenyl)diphenylsulfonium triflate
PEN	Poly(ethylene naphthalate)
PI	Polyimide
PMA	Phosphomolybdic acid
PVB	Poly(vinyl butyral)
PVP	Polyvinylpyrrolidone
RBBR	Remazol brilliant blue R
rGO	Reduced graphene oxide
SiO ₂	Silicon dioxide
TB	Thymol blue
Te	Tellurium
TiO ₂	Titanium dioxide
TST	Triphenylsulfonium triflate
ZnO	Zinc oxide

Supplementary References

- [1] W. Zou, M. Sastry, J. J. Gooding, R. Ramanathan, V. Bansal, *Adv. Mater. Technol.* **2020**, *5*, 1901036.
- [2] R. S. Veerla, P. Sahatiya, S. Badhulika, *J. Mater. Chem. C* **2017**, *5*, 10231.
- [3] Y. Zhang, W. Xu, X. Xu, W. Yang, S. Li, J. Chen, X. Fang, *Nanoscale Horiz.* **2019**, *4*, 452.
- [4] C.-H. Lin, D.-S. Tsai, T.-C. Wei, D.-H. Lien, J.-J. Ke, C.-H. Su, J.-Y. Sun, Y.-C. Liao, J.-H. He, *ACS Nano* **2017**, *11*, 10230.
- [5] X. Liu, L. Gu, Q. Zhang, J. Wu, Y. Long, Z. Fan, *Nat. Commun.* **2014**, *5*, 4007.
- [6] J. An, T.-S. D. Le, C. H. J. Lim, V. T. Tran, Z. Zhan, Y. Gao, L. Zheng, G. Sun, Y.-J. Kim, *Adv. Sci.* **2018**, *5*, 1800496.
- [7] X. Xu, J. Chen, S. Cai, Z. Long, Y. Zhang, L. Su, S. He, C. Tang, P. Liu, H. Peng, X. Fang, *Adv. Mater.* **2018**, *30*, 1803165.
- [8] C. Zhou, X. Wang, X. Kuang, S. Xu, *J. Micromech. Microeng.* **2016**, *26*.
- [9] P. S. Khiabani, M. B. Kashi, X. Zhang, R. Pardehkorram, B. P. Markhali, A. H. Soeriyadi, A. P. Micolich, J. J. Gooding, *Carbon* **2018**, *138*, 215.
- [10] D. Wen, Y. Liu, C. Yue, J. Li, W. Cai, H. Liu, X. Li, F. Bai, H. Zhang, L. Lin, *RSC Adv.* **2017**, *7*, 54741.
- [11] S. J. Kim, D.-I. Moon, M.-L. Seol, B. Kim, J.-W. Han, M. Meyyappan, *ACS Appl. Mater. Interfaces* **2018**, *10*, 40198.
- [12] S. J. Kim, J.-W. Han, B. Kim, M. Meyyappan, *ACS Sens.* **2017**, *2*, 1679.
- [13] N. Nasiri, R. Bo, T. F. Hung, V. A. L. Roy, L. Fu, A. Tricoli, *Adv. Funct. Mater.* **2016**, *26*, 7359.
- [14] S. Y. Heo, J. Kim, P. Gutruf, A. Banks, P. Wei, R. Pielak, G. Balooch, Y. Shi, H. Araki, D. Rollo, C. Gaede, M. Patel, J. W. Kwak, A. E. Peña-Alcántara, K.-T. Lee, Y. Yun, J. K. Robinson, S. Xu, J. A. Rogers, *Sci. Transl. Med.* **2018**, *10*, eaau1643.
- [15] T. Ahmed, S. Kuriakose, S. Abbas, M. J. S. Spencer, M. A. Rahman, M. Tahir, Y. Lu, P. Sonar, V. Bansal, M. Bhaskaran, S. Sriram, S. Walia, *Adv. Funct. Mater.* **2019**, *29*, 1901991.
- [16] A. Mills, K. McDiarmid, M. McFarlane, P. Grosshans, *Chem. comm.* **2009**, DOI: 10.1039/B900569B1345.
- [17] H. Araki, J. Kim, S. Zhang, A. Banks, K. E. Crawford, X. Sheng, P. Gutruf, Y. Shi, R. M. Pielak, J. A. Rogers, *Adv. Funct. Mater.* **2017**, *27*, 1604465.
- [18] P. S. Khiabani, A. H. Soeriyadi, P. J. Reece, J. J. Gooding, *ACS Sens.* **2016**, *1*, 775.
- [19] S. Khankaew, A. Mills, D. Yusufu, N. Wells, S. Hodgen, W. Boonsupthip, P. Suppakul, *Sens. Actuators B Chem.* **2017**, *238*, 76.
- [20] M. Qiu, P. Sun, Y. Liu, Q. Huang, C. Zhao, Z. Li, W. Mai, *Adv. Mater. Technol.* **2018**, *3*, 1700288.
- [21] J. Wang, A. S. Jeevarathinam, A. Jhunjhunwala, H. Ren, J. Lemaster, Y. Luo, D. P. Fenning, E. E. Fullerton, J. V. Jokerst, *Adv. Mater. Technol.* **2018**, *3*.
- [22] W. Zou, A. González, D. Jampaiah, R. Ramanathan, M. Taha, S. Walia, S. Sriram, M. Bhaskaran, J. M. Dominguez-Vera, V. Bansal, *Nat. Commun.* **2018**, *9*, 3743.

- [23] I. Norrbo, A. Curutchet, A. Kuusisto, J. Mäkelä, P. Laukkanen, P. Paturi, T. Laihinen, J. Sinkkonen, E. Wetterskog, F. Mamedov, T. Le Bahers, M. Lastusaari, *Mater. Horiz.* **2018**, *5*, 569.
- [24] J. Kim, G. A. Salvatore, H. Araki, A. M. Chiarelli, Z. Xie, A. Banks, X. Sheng, Y. Liu, J. W. Lee, K.-I. Jang, S. Y. Heo, K. Cho, H. Luo, B. Zimmerman, J. Kim, L. Yan, X. Feng, S. Xu, M. Fabiani, G. Gratton, Y. Huang, U. Paik, J. A. Rogers, *Sci. Adv.* **2016**, *2*, e1600418.
- [25] M. E. Lee, A. M. Armani, *ACS Sens.* **2016**, *1*, 1251.
- [26] V. L. Hingorani, R. Karnik, J. J. Lees (Microsoft Technology Licensing LLC) *Patent US9360364B2*, **2016**.
- [27] Y. Shi, R. Pielak, G. Balooch (L'oreal) *Patent WO2017120176A1*, **2017**.
- [28] P. WEI, R. Pielak, Y. Shi, E. MESSAGER, G. Balooch (L'OREAL) *Patent US20190204146A1*, **2018**.
- [29] E. Dumont, S. Banerjee, M. CONTRERAS *Patent US20160364131A1*, **2016**.
- [30] E. Likovich, K. J. Russell, T. C. Hayes, J. Olds, R. Schwartz (SunSprite) *Patent US9933298B2*, **2018**.
- [31] QSUN, QSun UV Exposure Tracker, <https://qsun.co/>, accessed: December 2022.
- [32] N. Sood, N. Gonzalez, E. Guadarrama (Stella Wearables Inc) *Patent US10072975B2*, **2018**.
- [33] J. Lian, N. Bennouri, N. Chaimanonart *Patent US 2015/0177058A1*, **2015**.
- [34] K. L. Edgett, S. Aslam, S. Potbhare (Sunfriend Corporation) *Patent US D715664S*, **2014**.
- [35] Y. Shi, M. Manco, D. Moyal, G. Huppert, H. Araki, A. Banks, H. Joshi, R. McKenzie, A. Seewald, G. Griffin, E. Sen-Gupta, D. Wright, P. Bastien, F. Valceschini, S. Seité, J. A. Wright, R. Ghaffari, J. Rogers, G. Balooch, R. M. Pielak, *PLoS One* **2018**, *13*, e0190233.
- [36] A. S. Levine, A. M. Levine, N. A. Zujovic (Jads International LLC) *Patent US9658101B1*, **2017**.
- [37] A. Mills, M. McFarlane, K. McDiarmid, P. Grosshans (Intellego Technologies AB) *Patent US9097588B2*, **2015**.
- [38] C. M. Sweeting, D. M. H. Jouppi, A. B. Martinko, M. W. Gibson, K. Q. V. D. T. Wu, C. S. Mills, S. C.-H. Chang (8996598 Canada INC) *Patent US20190041261A1*, **2019**.
- [39] P. Foller, I. Fritz, C. Olguin, S. Wrobel, C. L. Maitre, E. R. Kang, S. J. E. Tibbits (LogicInk Corporation) *Patent WO2018232387A1*, **2018**.